Carbon Trends 13 (2023) 100309

Contents lists available at ScienceDirect

Carbon Trends

journal homepage: www.elsevier.com/locate/cartre

Occurrence of natural fullerene C_{60} from the iridium-rich Cretaceous-Paleogene (K-Pg) boundary layers of the Um-Sohryngkew river section, Meghalaya, India

Bhaskar J. Saikia [a,*], G. Parthasarathy [b], Binoy K. Saikia [c], Rashmi R. Borah [d]

[a] Department of Physics, Anandaram Dhekial Phookan College, Nagaon 782002, India
[b] National Institute of Advanced Studies, School of Natural Sciences and Engineering, Indian Institute of Science Campus, Bengaluru 560012, India
[c] Coal and Energy Division, CSIR-North East Institute of Science and Technology, Jorhat 785006, India
[d] Department of Physics, Nowgong College (Autonomous), Nagaon 782001, India

ARTICLE INFO

Keywords:
Um-Sohryngkew river section
K-Pg boundary
Fullerene
Raman
Infrared

ABSTRACT

The presence of fullerene C_{60} in the iridium-rich Cretaceous-Palaeogene (K-Pg) boundary layer from the Um-Sohryngkew river section of Meghalaya is reported here for the first time. Different analytical methods, including transmission electron microscopy (TEM), Raman spectroscopy, Fourier transform infrared (FT-IR), and X-ray diffraction(XRD) techniques, have been used to characterize the presence of toluene-insoluble high-pressure phase of fullerene C_{60} in the acid resistant carbonaceous matter extracted from the Um-Sohryngkew river section, Meghalaya, India. Strong absorption peaks at wavenumbers 1427, 1181, 574, and 525 cm^{-1}, which are indicative of pristine fullerene C_{60}, can be seen in the FTIR spectroscopic study. The Raman spectrum also independently confirms the presence of fullerene, by exhibiting the characteristics peaks of pristine fullerene C_{60}. The XRD technique provides further, independent validation of fullerenes, and the XRD pattern demonstrates fullerene presence. Fullerenes, high-pressure fullerene, the amorphous phase of C_{60}, and iridium all coexist and offer conclusive proof of impact at the Cretaceous-Palaeogene (K-Pg) boundary extinction event.

1. Introduction

The Cretaceous–Palaeogene (K–Pg) boundary is the Earth's geological signature, usually a thin boundary layer formed at ~ 66.016 ± 0.050Ma. The identification of K–Pg boundary is primarily based on biozonation with marked changes in the benthic foraminiferal distribution [1]. Based on geochemical and mineral markers like high iridium anomalies, platinum group inter-element ratios, the presence of spherules, high pressure polymorphs of silica, Ni-rich spinel, traces of meteorite, most likely extraterrestrial helium, the presence of diamond, chemical-mineralogical characteristics of clay minerals, etc., over one hundred K-Pg boundary sections have been found worldwide [2,3]. Moreover, in geological environment and in major K-Pg boundaries, the presence of natural fullerene C_{60} were also reported [2–7]. The K-Pg boundary is identified by a characteristic layer of clay that is frequently substantially enriched in elements like iridium and osmium, other platinum group element (PGE) concentrations, total organic carbon (TOC), and the presence of spherules in comparison to the layers above and below [8]. There are three major K–Pg boundary sections are reported from India at the Deccan Volcanic Province, Um-Sohryngkew river section, Meghalaya and the Cauvery Basin. The Indian subcontinent dinosaur extinction occurred after the deposition of iridium-rich sediments [1]. According to geochronologic, paleomagnetic, and paleontologic constraints, the Deccan volcanic activity began within the uppermost 30 N Maastrichtian Chron, and ^{40}Ar-^{39}Ar dates indicated an age of 66.5–67 Ma [1,9,10]. At the Um-Sohrynkew section, the K-Pg boundary is indicated by a thin red clay layer and a thick limonitic layer (~1.5 cm thick) that are both enriched with Ir, Co, Ne, Os, Fe, Zn, Sb (by a factor of 4 to ~1200), Ni-rich spinels, and rare earth elements (by a factor of 1.7 to ~5) [11–15] and contain a lot of subangular quartz grains in a brown matrix [16]. The iridium profile at the K-Pg boundary at Um-Sohrynkew is about 12 ng/g, ten times higher than the background level [14]. The remarkable concentration of iridium was in accordance with the theory that these elements have extraterrestrial origins [17]. However, understanding the palaeoenvironmental, palaeoclimatic, and palaeodepositional conditions of the K-Pg boundary has

* Corresponding author.
E-mail address: vaskaradp@gmail.com (B.J. Saikia).

https://doi.org/10.1016/j.cartre.2023.100309
Received 22 July 2023; Received in revised form 28 October 2023; Accepted 31 October 2023
Available online 1 November 2023

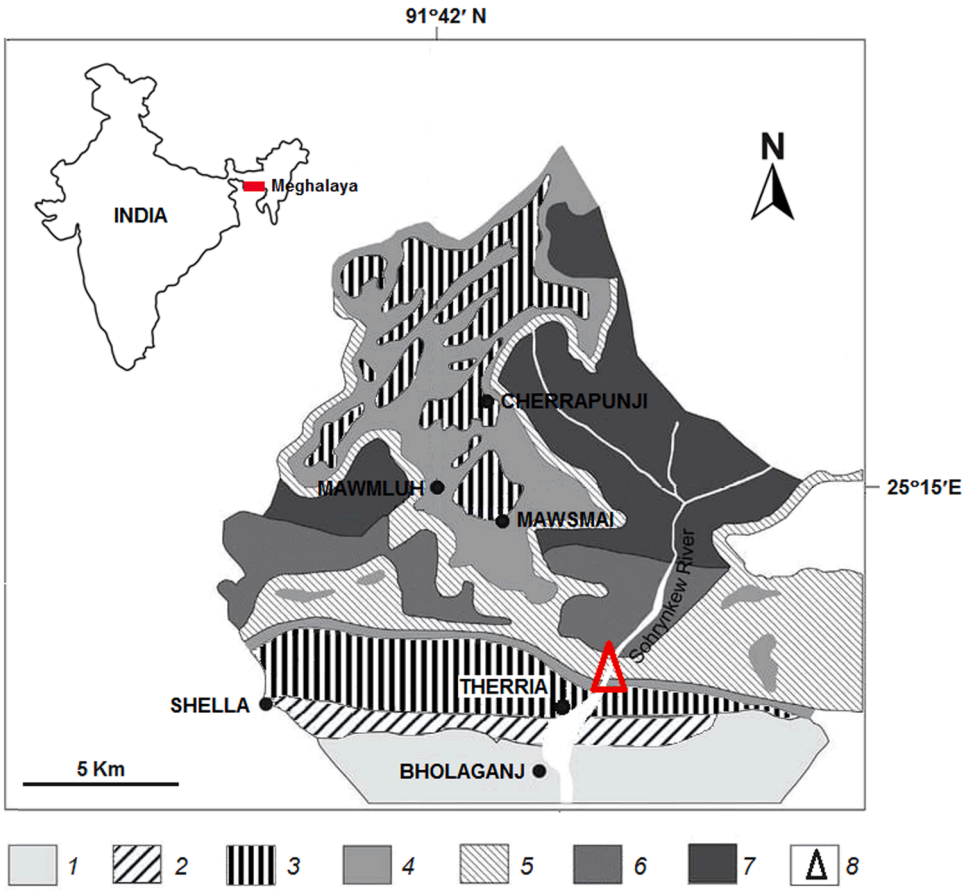

Fig. 1. The South Shillong Plateau in Meghalaya, Northeastern India, is depicted on a geological map in summary (modified after Tewari et al. [21,22]). 1. Alluvium; 2. Kopili formation (upper Eocene); 3. Lakadong, Prang and Umlatadoh formations (upper Paleocene to middle Eocene); 4. Therria formation (upper Paleocene); 5. Um Sohrynkew, Mahadek and Langpar formations (upper Cretaceous to lower Paleocene); 6. Sylhet Traps (Jurassic/Cretaceous); 7. Archean; 8. Location of the sample.

been accomplished using clay mineralogy. According to subsequent biostratigraphic research, the clay layer occurs below the real K-Pg boundary in the Um-Sohrynkew river segment [18–20]. This portion comprises of a continuous Campaniane Eocene succession typical of coastal, estuarine, and nearshore environments [21,22], with marine shelf deposits that contain thick sandstone layers, shale, marl, and carbonates [23]. In addition, there are also documented anomalies of enriched Au, Pt, and Pd in a brown clay layer comprising illite, kaolinite, montmorillonite, and illite/smectite mixed complexes that are found in this portion [24,25]. There was no previous report on the occurrence of fullerene in the Meghalaya K-Pg section. The first report on the natural fullerene from the K-Pg section of New Zealand has been reported from toluene extracts of samples from two Cretaceous-Tertiary (K-T) boundary sites in New Zealand has revealed the presence of C_{60} at concentrations of 0.1 to 0.2 parts per million of the associated soot [5]. A comprehensive review on occurrence of Fullerenes C_{60} and C_{70} in the thin clay seams of nine worldwide locations of the geologic boundary between the Cretaceous and Tertiary periods, has been discussed by Heymaan and Wolbach [26]. Fullerene occurrence and a rise in carbon soot content are thought to be significant geochemical indicators of the K-Pg boundary [3,6,27–30]. Earlier reports on fullerenes from India Anjar, Deccan Trap sections are reviewed by Partasarathy et al. [3]. Clay minerals have recently demonstrated a positive association between the adsorption of fullerenes and iridium in the K-Pg boundary section of the Anjar intertrappean beds, Kachchh, Gujarat, India [1]. Our present study represents the first report on the occurrence of natural fullerenes from the K-Pg boundary of the Um-Sohrynkew river section, Meghalaya, India. There were no data available in the literature on the details of the clay mineralogy and fullerenes from the studied geological section. The fullerene signatures can be used as a reliable geochemical indicator of impact metamorphism in terrestrial sediments by finding them at the K-Pg boundary of the Um-Sohrynkew river section.

1.1. Geological settings

The geological map of South Shillong Plateau, Meghalaya, Northeastern India is shown in the Fig. 1. The Shillong plateau consists of the Assam Meghalaya Gneissic Complex, meta-sedimentary rocks belonging to the Shillong Group, granite plutons, mafic igneous rocks, Sylhet Traps and ultramafic-alkaline carbonatite complex covered by the Cretaceous-Palaeogene sediments within the southernmost portion of the Meghalaya shelf [31]. The depositions of these sediments in Khasi Group are represented by the Jadukata and Mahadek Formations and in Jaintia Group are represented by the Langpar, Shella, and Kopili Formations. The Mahadek Formations are of the Late Cretaceous age and have a variety of lithologic characteristics, including coarse-grained gritstones, calcareous sandstones bearing glauconite, thin, fine-grained ferruginous limonitic sandstone, etc. The Langpar Formation of Jaintia Group is Late Cretaceous to Palaeocene in age and the calcareous shales with limestone bands in the Langpar Formation overlying the Mahadek Formation have yielded foraminifera. The Um-Sohryngkew river segment contains continuous marine sequences of Cretaceous to Paleocene age which includes four successive formations from bottom to the top: Mahadek, Langpar, Therria, and Lakadong. The foraminiferal assemblages from the Um- Sohryngkew, Therriaghat river section near Sohbar were used to record the Cretaceous-Palaeogene (K-Pg) boundary within the

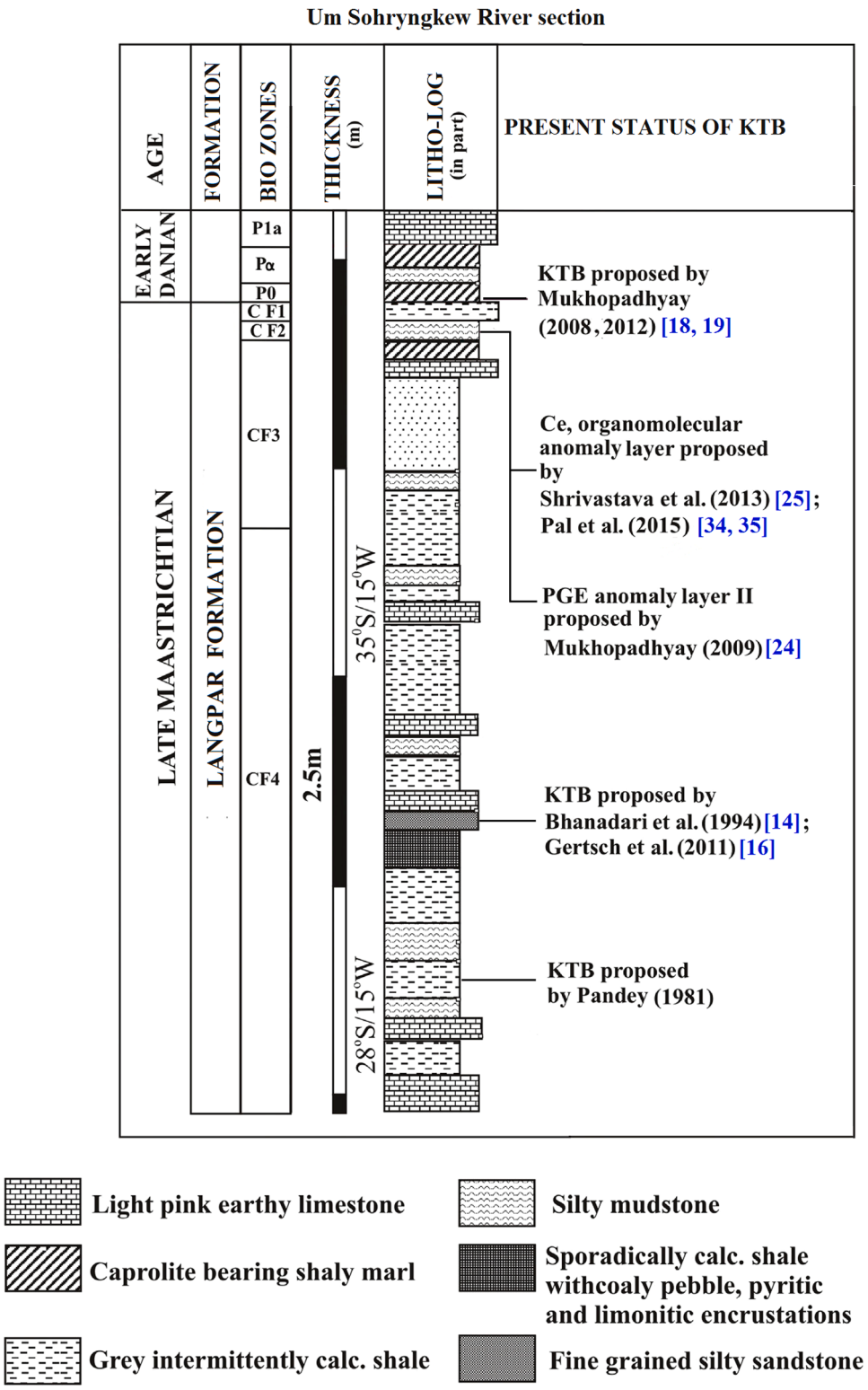

Fig. 2. Lithostratigraphy of the Um-Sohryngkew river section (modified after Mukhopadhyay [18]).

Langpar Formation [18]. The most comprehensive marine K-Pg succession known to exist anywhere in the world, including India, is included in this succession [16].

The lithostratigraphy of the Therriaghat section is shown in Fig. 2. The Langpar Formation is well exposed in this section on the west bank of the Um-Sohryngkew river. An inner shelf with an open marine connection and deepening during the Danian period is suggested by the lithological and foraminiferal assemblage [32]. However, the Langpar Formation contains a continuous K-Pg boundary section that is primarily made up of Precambrian meta-sediments and gneissic complexes. Based on the distribution of zonal indices, seven successive planktic foraminiferal zones have been identified at the K-Pg boundary at the Um-Sohrynkew river section [18,24,33–36]. These Palaeocene (P) biozones are Zone P0, Zone Pa, and Subzone P1a in the lower Danian part

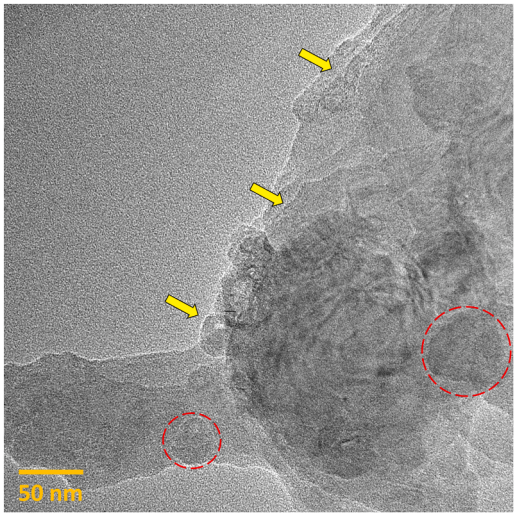

Fig. 3. TEM photograph showing that fullerene is a mixture of larger regular shaped fullerene particles and nearly spherical carbon black particles (Fullerene and carbon black are indicated by arrows and red dotted circles, respectively).

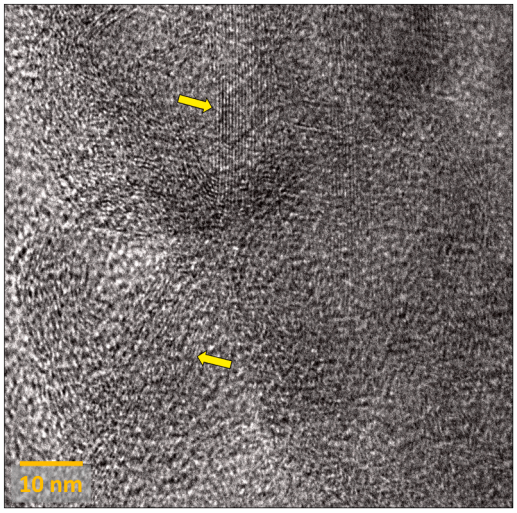

Fig. 4. TEM image showing the presence of graphitic layers within the amorphous region in the C_{60}-fullerene sample (indicated by arrow marks).

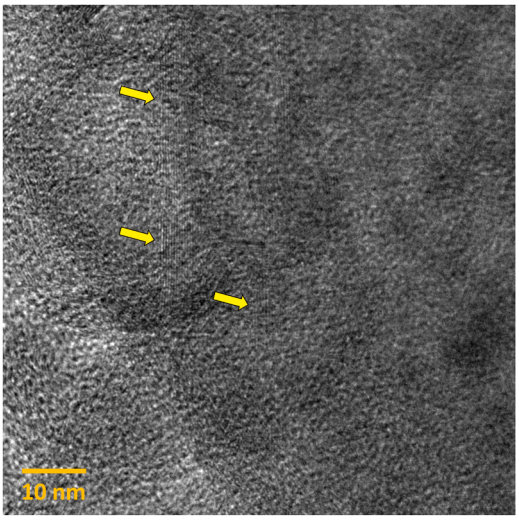

Fig. 5. TEM image showing the coexistence of graphitic layers with fullerenic carbons in the C_{60}-fullerene sample (indicated by arrow marks).

[37], and these Cretaceous Foraminifera (CF) biozones are CF4, CF3, CF2, and CF1 in the upper Maastrichtian part [38,39]. As a result, they represent a biostratigraphically continuous succession across the K-Pg boundary.

2. Experimental

After dispersion with a peptizing agent and ultrasonic treatment, the clay mineral fraction was eliminated by washing with double-distilled water. Sample preparation and extraction techniques are covered in detail elsewhere [3,40]. A standard acid-digestion technique was used to extract the carbonaceous material from the powdered sample [41,42]. The sample was treated for 24 h with 12 N HCl to remove the carbonates and then for 18 h with 60 % HF to remove silicates. The residue sample was then heated for an hour in 60 % HF at 70 °C to remove any traces of phyllosilicates. The resulting solid residue was then dried for an entire night at 80 °C after being washed with approximately one litre of double-distilled water. Toluene was used to extract the toluene-soluble fullerene C_{60} from a portion of the carbon-rich residues, which was then used for characterization.

High-resolution transmission electron microscopy (HRTEM) (JEOL, JEM-2100) was used to analyze the microstructure and particle sizes of the fullerene sample. For HRTEM analysis, the specimens were arranged by placing a drop of sample suspension on carbon-coated copper grids (300 μm) and letting it air-dry for overnight before analysis. The sample suspension was made by dissolving the fullerene in acetone solution.

Raman spectroscopy was used to analyze the structural properties and the presence of graphitic carbon in the fullerene sample. The Horiba Jobin Yvon Lab RAM-HR Micro Raman spectrometer was used to collect the Raman spectra. It was coupled with an Olympus microscope with 10x, 50x, and 100x objectives as well as a motorized x-y stage. A Nd: YAG laser with a power of 5 mW was used as the excitation source with wavelength 532 nm. The Raman spectra were collected in the range from 100 cm^{-1} to 3000 cm^{-1}.Throughout the experiment, Raman data were gathered at 28 °C ambient temperature. Counting times for spectral data collection typically ranged from 10 to 60 s.

The fullerene sample was analyzed using a Fourier transform-infrared (FT-IR) spectrophotometer (Model no. Spectrum Two, Make: PerkinElmer) in the transmission range of 4000–400 cm^{-1} with a 4 cm^{-1} spectral resolution to determine the surface functional groups. A small agate mortar was used to properly grind and combine the sample with KBr in a ratio of 1:40 mixture before creating the sample pellet. The absorption bands of the functional groups are evaluated by using the software associated with the system.

A fraction of the powered carbon-rich residue is used for X-ray diffraction technique using Philips PW 3710/31 (Philips, USA) diffractometer, scintillation counter, CuKα radiation and Ni filter at 40 kV and 35 mA. We used 2θ range of 10° to 80° with a step size of 0.02° and a count time of 0.5 s per step. The slits used consisted of 1° fixed divergence and anti scatter slits and a 0.2 mm receiving slit.

3. Results and discussion

The TEM photograph is shown in Fig. 3. In Fig. 3, a large irregular shaped and strongly aggregated mixture confirmed as fullerenes with nearly spherical carbon black particles. The size of the particles were varies over a broad range. An obvious difference in microstructure between different particles can be seen in the TEM image. Particles of fullerene were found to range in size from 110 to 120 nm on average. It is noteworthy that the smaller spherical particles seemed to be more clumped together than the fullerene. In addition to fullerene, the presence of both graphitic and amorphous carbon polymorphs has been

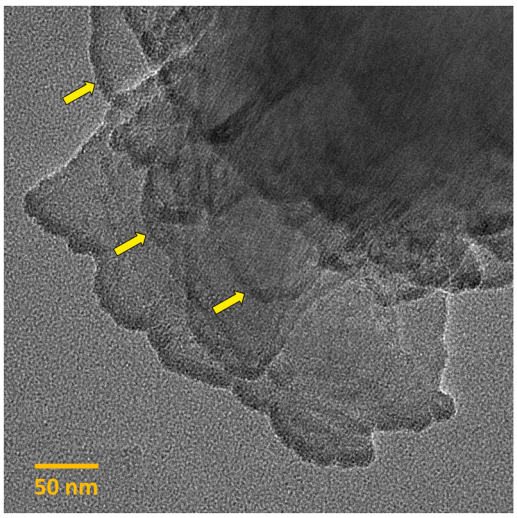

Fig. 6. TEM image showing that the particles are comprised of underdeveloped graphitic layers and are continuous from one to the other on the lattice scale (indicated by arrow marks).

observed in this sample. Fig. 4 reveals amorphous carbon associated with the deposited stacked graphitic layers. Moreover, coexistence of fullerene signature with graphitic layers is also observed. As seen in Fig. 5, the fullerenic carbons are embedded within the stacked planar graphitic layers. The stacked planar graphitic layers are seen to have equal amounts of amorphous carbon regions that have developed into the graphitic layers. Both mesopores and macropores were found together with the fullerene particles. The representative microstructure of carbon black, which is an intermediate structure between the amorphous and fully graphitized carbon, is shown in TEM images of a fullerene sample (Fig. 6). Around 3–5 graphitic layers can be next to each other at most. The high surface area of carbon blacks, according to Donnet et al. [43] consisted primarily of sp2-hybridized carbon atoms. The faces of graphitic sheets and the edges of these particles are typically heterogeneous [43].

Characterizing carbon-based materials can be done effectively with the help of Raman spectrometry. Raman spectrum of the studied sample is shown in Fig. 7. Generally, inter-molecular or lattice modes and intramolecular or molecular modes are the two main categories into which the vibrational modes of fullerene C_{60} can be divided. The latter mode of vibration, however, occurred at a higher frequency (above 270 to 1700 cm^{-1}), whereas the first mode of vibration occurred at lower frequencies. The Raman spectrum of pristine fullerene C_{60} shows characteristics peaks at 270, 431, 493, 708, 773, 1099, 1248, 1426, 1469, and 1572 cm^{-1} [44,45].The strongest and most significant peaks in the fullerene C_{60} spectrum were located at around 493 and 1469 cm^{-1}, and they were identified as the *Ag(1)* mode, which corresponds to the symmetrical radial breathing motion of the sixty carbon atoms, and the *Ag(2)* pentagonal pinch mode, which corresponds to the tangential stretching mode of the five-fold pentagon carbons [44–49]. The other peaks found at 270, 431, 708, 773, 1099, 1248, 1426, 1469, and 1572 cm^{-1} were correlated to *Hg*(1) to *Hg*(8) modes [44,45]. Herein the Raman spectrum clearly reproduces the 10 Raman modes. The Raman spectrum of studied natural fullerene C_{60} sample shows the peaks at 272, 403, 489, 710, 1425, 1467 and 1590 cm^{-1}. The sharpness of the bands pointed towards the uniform nature of the bonds. The D band indicates structural disorder or the presence of sp3 carbons. The G-band at 1590 cm^{-1} is comparable to the E_{2g} mode of graphitic domains or sp2-hybridized carbon matrix. The *Hg*(8) mode of pristine fullerene C_{60} is generally found at 1572 cm^{-1}, which is shifted to 1590 cm^{-1} in the studied sample. The absence of 1332 cm^{-1} peak in micro Raman indicates there is no nanodiamonds in this K-Pg section as reported in other K-Pg sections. However, one hypothesis for the origin of the nanometer-size diamonds observed at the K-Pg boundary is that they are relict interstellar diamond grains carried by a postulated asteroid [50].

The infrared absorption bands at around 528, 577, 1183, and 1429 cm^{-1} are attributed to pristine fullerene C_{60}, and the strong peaks at around 509 cm^{-1} and 740 cm^{-1} are typical of fullerene C_{60} in its high-pressure and high-temperature phases [51]. The infrared spectrum of the studied sample (Fig. 8) exhibits prominent fullerene peaks at 525, 574, 1181, and 1427 cm^{-1} attributed to C–C vibrational modes. With its incredibly high symmetry, it is accepted that the free, truncated icosahedral molecule exhibits these four strong peaks. The fullerene C_{60}, on the other hand, has the I_h point group symmetry, which is the highest symmetry of any known molecule. The icosahedral symmetry of the molecule leads to a number of degenerate modes despite the fullerene C_{60} molecule only having 46 vibrational modes distributed over the 174 vibrational degrees of freedom (3N-6) for each fullerene C_{60} molecule. Among these 46 vibrational modes ($2A_g + 3F_{1g} + 4F_{2g} + 6G_g + 8H_g + A_u + 4F_{1u} + 5F_{2u} + 6G_u + 7H_u$), only four are infrared-active ($4F_{1u}$) and ten are Raman-active ($2Ag + 8$ Hg), while the remaining modes are optically inactive [48,52–54]. Moreover, in the observed infrared spectrum of natural fullerene C_{60} containing four modes of F_{lu} symmetry: F_{1u} *(1),* F_{1u}

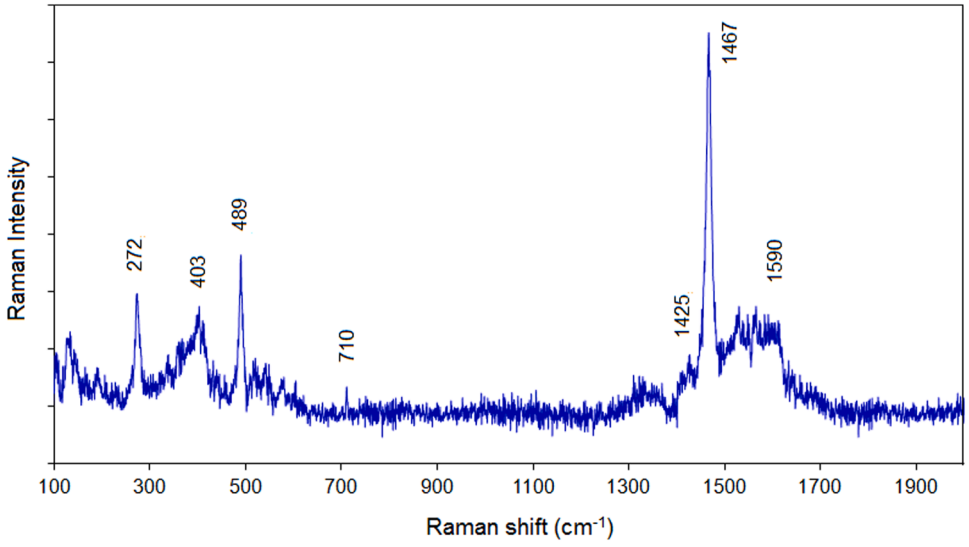

Fig. 7. Raman spectrum of fullerene C_{60} from Um-Sohrynkew river section in the range 100–2000 cm^{-1}.

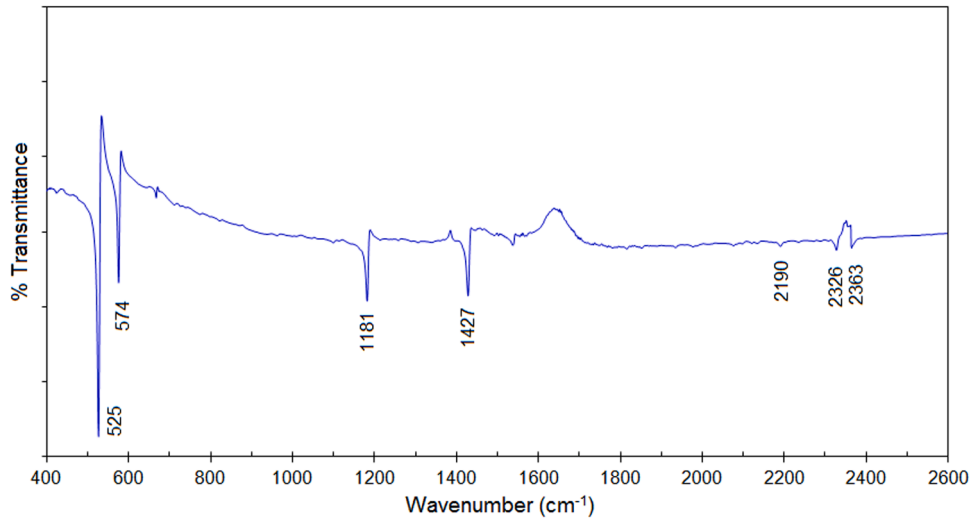

Fig. 8. Infrared spectrum of fullerene C_{60} from Um-Sohrynkew river section in the range 400–2600 cm^{-1}.

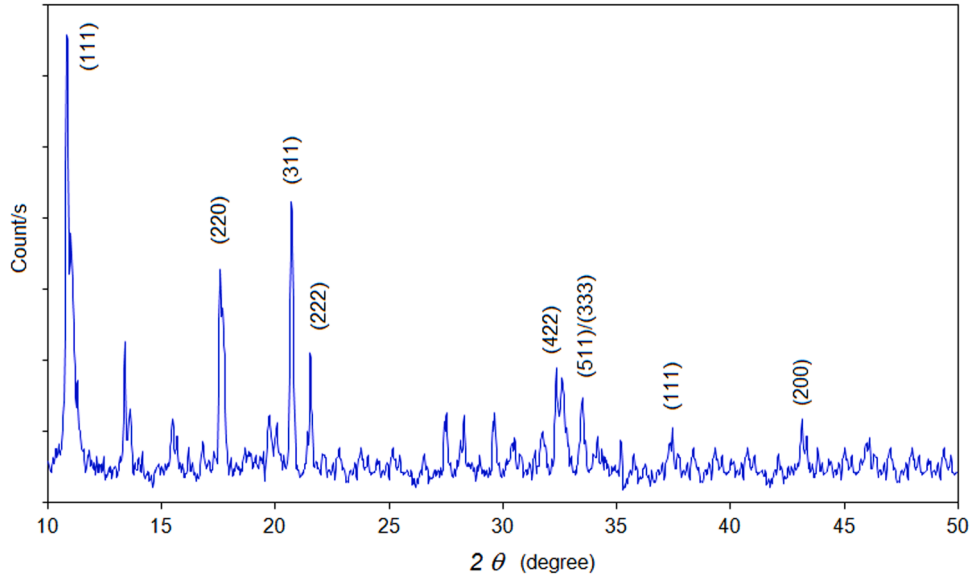

Fig. 9. X-ray diffraction pattern of fullerene C_{60} from Um-Sohrynkew river section.

(2), F_{1u} (3) and *F_{1u}(4)* corresponding to the frequencies at 525, 574, 1181 and 1427 cm^{-1}. All observed infrared active F_{lu} modes of the natural fullerene C_{60} are good agreement with quantum mechanical computations on the vibrational spectrum of fullerene [52–54]. The observed peaks at 527 and 574 cm^{-1} are assigned to radial displacements of the carbon atoms, whereas the other peaks at 1181 and 1427 cm^{-1} are correspond to the tangential modes of the carbon atoms [55]. The characteristic pentagonal pinch vibrational mode is observed at 1427 cm^{-1}. Traces of CO_2 and CO are indicated by weak bands at 2190, 2326, and 2363 cm^{-1} [3,51].

The X-ray diffraction pattern of the studied sample is shown in Fig. 9. The X-ray powder diffraction pattern is consistent with the Raman and infrared spectroscopic analysis. The (111), (220), (311), (222), (331), (420), (422) and (511)/(333) reflections, which originate from the fullerene C_{60} fcc lattice, are the most common eight reflections seen in X-ray powder diffraction studies of the molecular packing of the C_{60} superstructure [40,56–61]. The X-ray diffraction pattern of the studied natural fullerene sample exhibits peaks at 10.84°, 17.56°, 20.71°, 21.52°, 32.32°, and 33.42° as 2θ correspond to the (111), (220), (311), (222), (422), and (511)/(333) plans of the fullerene C_{60}.

4. Conclusion

This is the first proof that fullerene exists in the K-Pg boundary of the section of the Um-Sohrynkew River. Transmission electron microscopy, Raman spectroscopy, Fourier transform infrared spectroscopy, and X-ray diffraction studies have all confirmed the presence of pristine C60 fullerene phase in the iridium-enriched K-Pg boundary of the Um-Sohrynkew River section. High-pressure fullerene and amorphous phase are thought to be significant geochemical indicators of impact at the K-Pg boundary.

CRediT authorship contribution statement

Bhaskar J. Saikia: Conceptualization, Methodology, Formal analysis, Data curation, Supervision, Investigation, Writing – original draft, Writing – review & editing. **G. Parthasarathy:** Conceptualization, Methodology, Supervision, Writing – review & editing. **Binoy K. Saikia:** Investigation, Data curation. **Rashmi R. Borah:** Methodology, Formal analysis, Data curation.

Declaration of Competing Interest

The authors declare that they have no known competing financial interests or personal relationships that could have appeared to influence the work reported in this paper.

Data availability

The authors do not have permission to share data.

Acknowledgments

We are grateful to the anonymous reviewers for their constructive comments, which have improved this manuscript. We thank Directors, CSIR- North East Institute of Science and Technology, Jorhat, and Indian Institute of Technology, Guwahati (IITG) for providing analytical facilities for characterization of the sample. We thank Dr. S. Sarmah, IIT Guwahati for his assistance in the spectroscopic analysis. We also thank Abhishek Hazarika, CSIR-NEIST, Jorhat for his assistance in TEM analysis. We are grateful to Professor N. Bhandari for his kind encouragements and guidance. GP is grateful to National Institute of Advanced Studies and Indian National Science Academy for their support.

References

[1] P. Roy, G. Parthasarathy, B. Bulusu Sreenivas, Clay minerals and the adsorption of fullerenes: clues from iridium-enriched Cretaceous–Palaeogene Anjar intertrappean beds, Kachchh district, Gujarat, India, Curr. Sci. 124 (2023) 87–93, https://doi.org/10.18520/cs/v124/i1/87-93.

[2] G. Keller, T. Adatte, W. Stinnesbeck, D. Stueben, Z. Berner, Age-chemo- and biostratigraphy of Haiti spherule rich deposits: a multi-event K-T-scenario, Can. J. Earth Sci. 38 (2001) 197–227, https://doi.org/10.1139/e00-087.

[3] G. Parthasarathy, N. Bhandari, M. Vairamani, A.C. Kunwar, High-pressure phase of natural fullerene C60 in iridium-rich Cretaceous–Tertiary boundary layers of Deccan intertrappean deposits, Anjar, Kutch, India, Geochim. Cosmochim. Acta 72 (2008) 978–987, https://doi.org/10.1016/j.gca.2007.12.003.

[4] P.R. Buseck, J.T. Semeon, R. Hettich, Fullerenes from the geological environment, Science 257 (1992) 215, https://doi.org/10.1126/science.257.5067.215.

[5] D. Heymann, L.P.F. Chibante, P.R. Brooks, W.S. Wolbach, R.E. Smalley, Fullerenes in the K/T boundary layer, Science 265 (1994) 645–647, https://doi.org/10.1126/science.265.5172.645.

[6] D. Heymann, L.P.F. Chibante, P.R. Brooks, W.S. Wolbach, J. Smit, A. Korochantsev, M.A. Nazarov, R.E. Smalley, G. Ryder, D. Fastovsky, S. Garter, Fullerenes of possible wildfire origin in Cretaceous–Tertiary boundary sediments, in: The Cretaceous–Tertiary Event and Other Catastrophes in Earth History, 307, Geological Society of America Special Paper, 1996, pp. 455–464.

[7] D. Heymann, T.E. Yancey, W.S. Wolbach, M.H. Thiemens, E.A. Jhonson, D. Roach, S. Moecker, Geochemical markers of the Cretaceous–Tertiary boundary event at Brazos River, Texas, USA, Geochim. Cosmochim. Acta 62 (1998) 173–181, https://doi.org/10.1016/S0016-7037(97)00330-X.

[8] Z. Li, H. Hong, L. Liao, H. He, X-ray diffraction and trace element analyses of K/Pg boundary samples collected from Agost and Caravaca, Spain, Crystals 13 (2023) 670, https://doi.org/10.3390/cryst13040670.

[9] C.J. Sprain, P.R. Renne, L. Vanderkluysen, K. Pande, S. Self, T. Mittal, The eruptive tempo of Deccan volcanism in relation to the Cretaceous-Paleogene boundary, Science 363 (2019) 866–870, https://doi.org/10.1126/science.aav1446.

[10] B. Schoene, M.P. Eddy, K.M. Samperton, C.B. Keller, G. Keller, T. Adatte, S.F. R. Khadri, U-Pb constraints on pulsed eruption of the Deccan Traps across the end-Cretaceous mass extinction, Science 363 (2019) 862–866, https://doi.org/10.1126/science.aau2422.

[11] J. Pandey, Cretaceous/Tertiary boundary, iridium anomaly and foraminifer breaks in the Um Sohryngkew River section, Curr. Sci. 59 (1990) 570–575.

[12] N. Bhandari, P.N. Shukla, J. Pandey, Iridium enrichment at Cretaceous-Tertiary boundary in Meghalaya, Curr. Sci. 56 (1987) 1003–1005.

[13] N. Bhandari, P.N. Shukla, G.C. Castognoli, Geochemistry of some K/T sections in India, Palaeogeogr. Palaeoclimatol. Palaeoecol. 104 (1993) 199–211, https://doi.org/10.1016/0031-0182(93)90131-2.

[14] N. Bhandari, M. Gupta, J. Panday, P.N. Shukla, Chemical profiles in K/T boundary section of Meghalaya, India: cometary, asteroidal or volcanic, Chem. Geol. 113 (1994) 45–60, https://doi.org/10.1016/0009-2541(94)90004-3.

[15] R. Garg, K. Ateequzzaman, V. Prasad, Significant dinoflagellate cyst biohorizons in the Upper Cretaceous–Paleocene succession of the Khasi Hills, Meghalaya, J. Geol. Soc. India 67 (2006) 737–747.

[16] B. Gertsch, G. Keller, T. Adatte, R. Garg, V. Prasad, Z. Berner, D. Fleitmann, Environmental effects of Deccan volcanism across the Cretaceous–Tertiary transition in Meghalaya, India, Earth Planet. Sci. Lett. 310 (2011) 272–285, https://doi.org/10.1016/j.epsl.2011.08.015.

[17] P.R. Renne, A.L. Deino, F.J. Hilgen, K.F. Kuiper, D.F. Mark, W.S. Mitchell, L. E. Morgan, R. Mundil, J. Smit, Time scales of critical events around the Cretaceous-Paleogene boundary, Science 339 (2013) 684–687, https://doi.org/10.1126/science.1230492.

[18] S.K. Mukhopadhyay, Planktonic for aminiferal succession in late Cretaceous to early Palaeocene strata in Meghalaya, India, Lethaia 41 (2008) 71–84, https://doi.org/10.1111/j.1502-3931.2007.00043.x.

[19] S.K. Mukhopadhyay, Guembelitria (Foraminifera) in the Upper Cretaceous-Lower Paleocene succession of the Langpar Formation, India, and its paleoenvironmental implication, J. Geol. Soc. India 79 (2012) 627–651.

[20] S.K. Mukhopadhyay, Planktonic foraminiferal zonation and sea-level changes in the upper Maastrichtian-middle Danian successions of Meghalaya, India, Stratigraphy 13 (2017) 245–276.

[21] V.C. Tewari, K. Lokho, K. Kumar, N.S. Siddaiah, Late CretaceousPaleocene Basin architecture and evolution of the Shillong Shelf sedimentation, Meghalaya, Northeast India, J. Indian Geol. Congr. 22 (2010) 61–73.

[22] V.C. Tewari, K. Kumar, K. Lokho, N.S. Siddaiah, Lakadong Limestone: paleocene-Eocene boundary carbonate sedimentation in Meghalaya, northeastern India, Curr. Sci. 98 (2010) 88–94.

[23] A.N. Sial, J. Chen, L.D. Lacerda, R. Frei, V.C. Tewari, M.K. Pandit, C. Gaucher, V. P. Ferreira, S. Cirilli, S. Peralta, C. Korte, J.A. Barbosa, N.S. Pereira, Mercury enrichment and Hg isotopes in Cretaceouse Paleogene boundary successions: links to volcanism and palaeoenvironmental impacts, Cretac. Res. 66 (2016) 60–81, https://doi.org/10.1016/j.cretres.2016.05.006.

[24] S.K. Mukhopadhyay, Convener's report for 2008 on the progress of work in the IGCP Project 507 on 'Palaeoclimate in Asia during the Cretaceous: their variations, causes, and biotic and environmental responses', IGCP India Newsletter 29(2009) 11–13.

[25] J.P. Shrivastava, S.K. Mukhopadhyay, S. Pal, Chemico-mineralogical attributes of clays from the late cretaceouse early Palaeogene succession of the Um Sohryngkew river section of Meghalaya, India: palaeoenvironmental inferences and the K/Pg boundary, Cretac. Res. 45 (2013) 247–257, https://doi.org/10.1016/j.cretres.2013.04.010.

[26] D. Heymann, W.S. Wolbach, Fullerenes in the Cretaceous-Tertiary boundary, in: Natural Fullerenes and Related Structures of Elemental Carbon. Developments in Fullerene Science, 6, Springer, Dordrecht, 2006, pp. 191–212, https://doi.org/10.1007/1-4020-4135-7_9.

[27] D. Heymann, W.S. Wolbach, L.P.F. Chibante, P.R. Brooks, R.E. Smalley, Search for extractable fullerenes in clays from the Cretaceous/Tertiary boundary of the Woodside Creek and Flaxbourne river sites, New Zealand, Geochim. Cosmochim. Acta 58 (1994) 3531–3534, https://doi.org/10.1016/0016-7037(94)90105-8.

[28] D. Heymann, W.S. Wolbach, Fullerenes in the Cretaceous-Tertiary boundary, in: Natural Fullerenes and Related Structures of Elemental Carbon. Developments in Fullerene Science, 6, Springer, Dordrecht, 2006, https://doi.org/10.1007/1-4020-4135-7_9.

[29] G. Parthasarathy, N. Bhandari, M. Vairamani, A.C. Kunwar, B. Narasaiah, Natural fullerenes from the Cretaceous-Tertiary boundary layer at Anjar, Kutch, India, Geological Society of America Special Papers 356(2002) 345–350, 10.1130/0-8137-2356-6.345.

[30] G. Parthasarathy, M. Vairamani, Testing for fullerenes in geologic materials: oklo carbonaceous substances, Karelian shungites, Sudbury Black Tuff: comment and Reply, Geology (2003) e32–e33, https://doi.org/10.1130/0091-7613-31.1.e32.

[31] B. Iangrai, L. Dalabehera, D. Mukherjee, A report on the late Cretaceous-early Palaeocene molluscs and echinoids from the Meghalaya shelf in the vicinity of the K-Pg Mass Extinction Boundary, J. Palaeontol. Soc. India 67 (2022) 285–309.

[32] S. Pal, J.P. Shrivastava, Cretaceous/Palaeogene boundary transition induced lattice defects in illite and kaolinite associated with the Um-Sohryngkew river section, Meghalaya, India, Solid Earth Sci. 5 (2020) 202–222, https://doi.org/10.1016/j.sesci.2020.06.004.

[33] S.K. Mukhopadhyay, R. Venkatchalapathy, Can late Maastrichian planktonic foraminifera and palaeoclimatic help understand the problems of Present Day global warming?. Earth Resource and Environment Research Publishing, Singapore, 2011, pp. 193–205.

[34] S. Pal, J.P. Shrivastava, S.K. Mukhopadhyay, Mineral chemistry of clays associated with the late Cretaceous-early Palaeogene succession of the Um Sohryngkew river section of Meghalaya: palaeoenvironmental inferences and K/Pg transition, J. Geol. Soc. India 86 (2015) 631–647.

[35] S. Pal, J.P. Shrivastava, S.K. Mukhopadhyay, Polycyclic Aromatic Hydrocarbon compound excursions and K/Pg transition in the late Cretaceous-early Paleogene succession of the Um-Sohryngkew River section, Meghalaya, Curr. Sci. 109 (2015) 1140–1150.

[36] S. Pal, K.M. Singamshetty, J.P. Shrivastava, S.K. Mukhopadhyay, S. Hamilton, Evidence of biotic recovery through the Cretaceous/Palaeogene transition from the Mahadeo-Cherrapunji succession in the Meghalaya shelf, India, Palaeobiodivers. Palaeoenviron. 103 (2023) 221–247, https://doi.org/10.1007/s12549-022-00534-2.

[37] W.A. Berggren, P.N. Pearson, A revised tropical to subtropical Paleogene planktonic foraminiferal zonation, J. Foraminifer. Res. 35 (2005) 279–298, https://doi.org/10.2113/35.4.279.

[38] L. Li, G. Keller, Maastrichtian climate, productivity and faunal turnovers in planktic foraminifera in south Atlantic DSDP 525a and 21, Mar. Micropaleontol. 33 (1998) 55–86, https://doi.org/10.1016/S0377-8398(97)00027-3.

[39] L. Li, G. Keller, Abrupt deep-sea warming at the end of the Cretaceous, Geology 11 (1998) 995–998.

[40] G. Parthasarathy, R. Srinivasan, M. Vairamani, K. Ravikumar, A.C. Kunwar, Occurrence of natural fullerenes in low-grade metamorphosed Proterozoic

shungites from Karelia, Russia, Geochim. Cosmochim. Acta 62 (1998) 3541–3544, https://doi.org/10.1016/S0016-7037(98)00242-7.
[41] K.W. Wedeking, J.M. Hayes, U. Matzigkeit, J.W. Schopf, Procedures of organic geochemical analysis. Earth's Earliest Biosphere: its Origin and Evolution, Princeton University Press, Princeton, USA, 1983, pp. 428–441.
[42] S.J. William, K. Cornelis, The Proterozoic Biosphere: a Multidisciplinary Study, Cambridge University Press, Cambridge, 1992.
[43] J.B. Donnet, R.C. Bansal, M.J. Wang, Carbon Black Science and Technology, Dekker, New York, 1993 second ed.
[44] M.S. Dresselhaus, G. Dresselhaus, P.C. Eklund, Raman scattering in fullerenes, J. Raman Spectrosc. 27 (1996) 351–371.
[45] M.S. Dresselhaus, G. Dresselhaus, P.C. Eklund, A.M. Rao, Carbon nanotubes, W. Andreoni, in: The Physics of Fullerene-Based and Fullerene-Related Materials. Physics and Chemistry of Materials with Low-Dimensional Structures, 23, Springer, Dordrecht, 2000, pp. 331–379.
[46] D.S. Bethune, G. Meijer, W.C. Tang, H.J. Rosen, The vibrational Raman spectra of purified solid films of C_{60} and $C_{70,}$ Chem, Phys. Lett. 174 (1990) 219–222, https://doi.org/10.1016/0009-2614(90)85335-A.
[47] W. Kraetschmer, L.D. Lamb, K. Fostiropoulos, D.R. Huffman, Solid C_{60}: a new form of carbon, Nature 347 (1990) 354–358, https://doi.org/10.1038/347354a0.
[48] H. Kuzmany, R. Pfeiffer, M. Hulman, C. Kramberger, Raman spectroscopy of fullerenes and fullerene–nanotube composites, Philos. Trans. R. Soc. Lond. Ser. A 362 (2004) 2375–2406, https://doi.org/10.1098/rsta.2004.1446.
[49] M. Sathish, K. Miyazawa, Synthesis and characterization of fullerene nanowhiskers by liquid-liquid interfacial precipitation: influence of C60 solubility, Molecules 17 (2012) 3858–3865, https://doi.org/10.3390/molecules17043858.
[50] I. Gilmour, S.S. Russell, J.W. Arden, M.R. Lee, I.A. Franchi, C.T. Pillinger, Terrestrial carbon and nitrogen isotopic ratios from Cretaceous-Tertiary boundary nanodiamonds, Science 258 (1992) 1624–1626, https://doi.org/10.1126/science.258.5088.1624.
[51] W. Kraetschmer, L.D. Lamb, K. Fostiropoulos, D.R. Huffman, Solid C_{60}: a new form of carbon, Nature 347 (1990) 354–358, https://doi.org/10.1038/347354a0.
[52] H. Kuzmany, R. Winkler, T. Pichler, Infrared spectroscopy of fullerenes, J. Phys. Condens. Matter 7 (1995) 6601–6624, https://doi.org/10.1088/0953-8984/7/33/003.
[53] V. Schettino, M. Pagliai, L. Ciabini, G. Cardini, The vibrational spectrum of fullerene C60, J. Phys. Chem. 105 (2001) 11192–11196, https://doi.org/10.1021/jp012874t.
[54] S. Iglesias-Groth, F. Cataldo, A. Manchado, Infrared spectroscopy and integrated molar absorptivity of C60 and C70 fullerenes at extreme temperatures, Mon. Not. R. Astron. Soc. 413 (2011) 213–222, https://doi.org/10.1111/j.1365-2966.2011.18124.x.
[55] H.W. Kroto, A.W. Allaf, S.P. Balm, C_{60} – Buckminsterfullerene, Chem. Rev. 91 (1991) 1213–1235, https://doi.org/10.1021/cr00006a005.
[56] K. Miyazawa, A. Obayashi, M. Kuwabara, C_{60} Nanowhiskers in a mixture of lead zirconate titanate Sol–C_{60} toluene solution, J. Am. Ceram. Soc. 84 (2001) 3037–3039, https://doi.org/10.1111/j.1151-2916.2001.tb01133.x.
[57] K. Miyazawa, Y. Kuwasaki, A. Obayashi, M. Kuwabara, C_{60} nanowhiskers formed by the liquid–liquid interfacial precipitation method, J. Mater. Res. 17 (2002) 83–88, https://doi.org/10.1557/JMR.2002.0014.
[58] K. Miyazawa, J.I. Minato, T. Yoshii, M. Fujino, T. Suga, Structural characterization of the fullerene nanotubes prepared by the liquid-liquid interfacial precipitation method, J. Mater. Res. 20 (2005) 688–695, https://doi.org/10.1557/JMR.2005.0091.
[59] J. Minato, K. Miyazawa, Solvated structure of C_{60} nanowhiskers, Carbon 43 (2005) 2837–2841, https://doi.org/10.1016/j.carbon.2005.06.013.
[60] L. Wang, B. Liu, D. Liu, M. Yao, Y. Hou, S. Yu, T. Cui, D. Li, G. Zau, A. Iwasiewicz, B. Sundqvist, Synthesis of thin, rectangular C_{60} nanorods using *m*-Xylene as a shape controller, Adv. Mater. 18 (2006) 1883–1888, https://doi.org/10.1002/adma.200502738.
[61] L. Wang, B. Liu, S. Yu, M. Yao, D. Liu, Y. Hou, T. Cui, G. Zau, B. Sundqvist, H. You, D. Zhang, D. Ma, Highly enhanced luminescence from single-crystalline C_{60}·1*m*-xylene nanorods, Chem. Mater. 18 (2006) 4190–4194, https://doi.org/10.1021/cm060997q.